

## New photoluminescence line-series spectra attributed to decay of multiexciton complexes bound to Li, B, and P centers in Si<sup>†</sup>

K. Kosai\* and M. Gershenson

Department of Materials Science and Electrical Engineering, University of Southern California, Los Angeles, California 90007

(Received 24 August 1973)

Pokrovskii and co-workers, in their photoluminescence studies of electron-hole liquid drops (EHD) in Si, observed, in doped samples at 2 K, three new lines associated with B and two with P. They speculated that the new lines, which were located several meV below the bound-exciton (BE) line of the related impurity, were due to radiative recombination within complexes consisting of several excitons bound to the impurity, and that these complexes resulted in nucleation of EHD. We have performed the first detailed studies of these new lines (designated here as  $b$  lines) and in addition to the lines previously reported by Pokrovskii *et al.* have observed two P and seven (possibly ten) Li  $b$  lines. For the three impurities (B, P, Li) studied, we have shown that the  $b$  lines, together with the BE line, form a series whose line energies,  $E_n$ , vary as  $E_n = E_{FE}(\text{effective}) - b(n + 1/2)^{1/2}$ , where  $n$  is the line number and begins with the BE line as number zero, and the values of  $E_{FE}(\text{effective})$  and  $b$  depend on the impurity. We have also correlated the photoluminescence intensities with impurity concentration and excitation intensity and performed time-resolved spectroscopy. The model most consistent with our experimental results is that of multiexciton complexes where line  $b_n$  arises from the decay of an exciton in an  $(n + 1)$ -exciton complex bound to an impurity, leaving the center in an  $n$ -exciton state.

### I. INTRODUCTION

The role of excitons in the near-band-gap absorption and radiative-recombination processes in Si are well understood. In pure material at low temperatures the free exciton (FE) in cooperation with momentum-conserving phonons has been shown to be responsible for the edge absorption<sup>1-3</sup> and photoluminescence.<sup>2,4,5</sup> Silicon containing  $10^{16}$ – $10^{17}$  cm<sup>-3</sup> of a group-III or -V impurity has been studied in photoluminescence (PL) at  $T \geq 15$  K and shows sharp lines due to the decay of excitons bound to neutral donors or acceptors.<sup>5,6</sup> These bound excitons (BE) have also been observed in absorption at 2 K and the oscillator strengths of the BE transitions have been measured.<sup>7</sup> Recently there has been considerable interest concerning a broad band observed only at  $T \leq 10$  K and originally attributed by Haynes to radiative recombination of the excitonic molecule.<sup>8-10</sup> Following a suggestion by Keldysh<sup>11</sup> the luminescence has been reinterpreted as recombination within a new electronic phase consisting of electrons and holes condensed into drops of a metallic liquid.<sup>12-15</sup> A similar broad band has been observed and extensively studied in Ge.<sup>15-18</sup>

Since the formation of electron-hole drops (EHD) is considered to be a first-order phase transition<sup>18</sup> in which the EHD condense from a vapor phase of excitons, Pokrovskii and co-workers hypothesized that EHD should initially nucleate at impurities.<sup>12-15</sup> He studied photoluminescence spectra of B-doped Si at 2 K and observed three new lines occurring at 1.0903, 1.0881, and 1.0863 eV on the low-energy side of the 1.0924-eV TO replica of the B BE.<sup>12-15</sup> He also reported two additional lines at

1.1465 and 1.144 eV near the no-phonon (NP) component of the P BE at 1.150 eV in samples doped with P.<sup>15</sup> He noted in the B-doped Si that as the excitation intensity increased, a tail appeared on the low-energy side of the new lines. As the excitation was further increased a broad band developed and gradually shifted to lower energies until it coincided in shape and peak energy with the luminescence attributed to the EHD. Pokrovskii and co-workers speculated that these new lines (which we designate as  $b$  lines) are due to the formation of multiexciton complexes at B atoms and that as the excitation is increased these lines broaden due to interactions with the EHD and eventually merge to form the broad EHD band.<sup>12-15</sup>

Presented here is the first investigation into the detailed mechanism responsible for the  $b$  lines in Si doped with B, P and Li. PL spectra due to isolated Li interstitial donors, the shallowest donor known in Si,<sup>19</sup> are reported here for the first time. It is shown that the spectra are consistent with the very small central-cell correction of the Li donor and with the trends previously observed for the group-III and -V impurities.<sup>5</sup> The majority of the experiments on the  $b$  lines were performed with the Li-doped samples since the Li  $b$  lines were the strongest and most numerous of the three impurities studied. Among experiments performed were gross temperature dependence, effects of impurity concentration and excitation intensity, and time-resolved spectroscopy.<sup>20</sup>

### II. EXPERIMENTAL

The Si used for these experiments was commercially grown by the float-zone, Czochralski or Lopek methods with no systematic differences no-

ticed in their PL. Lithium-doped samples were prepared only from float-zone Si of 500  $\Omega$  cm or higher resistivity by diffusion at 400–600  $^{\circ}$ C in dry argon. The impurity concentration was obtained from the sample resistivity by using published resistivity curves.<sup>21</sup> Since the PL efficiency of Si is known to be sensitive to the condition of the surface,<sup>5,22</sup> the samples were cleaned, etched lightly in a 5:3 solution of HNO<sub>3</sub> (70%) and HF (48%),<sup>22</sup> rinsed in deionized water and steamed for  $\sim$ 5 min<sup>2,5</sup> immediately before placing in the cold Dewar. The PL spectra were taken with the samples immersed in liquid He or cooled by cold gas boiled off from liquid He.<sup>23</sup> Whenever possible, sample temperatures were estimated from the shape and width of the FE luminescence bands,<sup>20</sup> but the temperatures derived in this manner are probably  $\sim$ 2–3 K high since there is broadening by nonthermal processes.<sup>1,2</sup> Photoexcitation sources used were a 200-W dc high-pressure mercury arc lamp and a pulsed GaAs cryogenic-laser-diode array. After the radiation from the arc lamp was filtered by 5 cm of CuSO<sub>4</sub> solution (13-g CuSO<sub>4</sub> · 5H<sub>2</sub>O + 50 mliter concentrated H<sub>2</sub>SO<sub>4</sub> + 1-liter deionized water)<sup>24</sup> and two Corning 1-75 filters, the total power onto the sample was approximately 1 W. The GaAs laser (RCA C30020) produced 42-W peak in a 2- $\mu$ sec pulse at 6-A drive with a duty factor of 4%. The peak generation rate in the Si is calculated to be  $1.7 \times 10^{26}$  electron-hole pairs/cm<sup>3</sup> sec for the laser, and  $4.5 \times 10^{24}$  pairs/cm<sup>3</sup> sec for the mercury arc, the latter being an experimental estimate which is discussed in Sec. III with the excitation experiments. The PL was taken from the irradiated side of the sample, analyzed with an f/8 Perkin-Elmer E-1 monochromator

which had a dispersion of 14  $\text{\AA}/\text{mm}$  in the 1- $\mu\text{m}$  region, detected by a cooled RCA 7102 photomultiplier and the resulting signal processed with either a lock-in amplifier or boxcar integrator. We estimate that at a 600-Hz chopping frequency the noise-equivalent power of the monochromator-photomultiplier combination was  $\sim 10^5$  photons/sec Hz<sup>1/2</sup> for 1.155 eV photons.

### III. RESULTS

The liquid-He PL spectra due to B, P, and Li in Si are shown in Figs. 1–3 with the peak energies of the lines listed in Tables I–III. Each line is labeled with the chemical symbol of the associated impurity, where the subscript indicates the phonon emitted and the notation in parentheses is the type of transition. The *b* lines are numbered consecutively to lower energies beginning with the highest-energy line closest to the BE line. We have observed P BE and *b* lines in samples doped to  $\sim 10^{16}$  cm<sup>-3</sup>, which together with Fig. 1 has enabled us to identify the lines in Fig. 2. In addition to the three B and two P *b* lines previously reported,<sup>15</sup> Figs. 2 and 3 show two new P and seven (possibly ten) Li *b* lines. There are also two weak lines, *a*<sub>1</sub> and *a*<sub>2</sub>, located on the low-energy side of P<sub>NP</sub> (BE) which are associated with P but these are always too weak to study.

The peak energies of the *b* lines are proportional to the square root of the line number *n*, as shown in Fig. 4, where  $E_{\text{FE}} - E_n$  is plotted vs  $n^{1/2}$  for Li and P with the BE taken as line number zero. The peak energies  $E_n$  are the NP values for P (Table II) and the TO values for Li (Table III), the last three Li lines being uncertain. The FE-emission thresholds,  $E_{\text{FE}}$  [1.1543 eV(NP) and 1.0963 eV

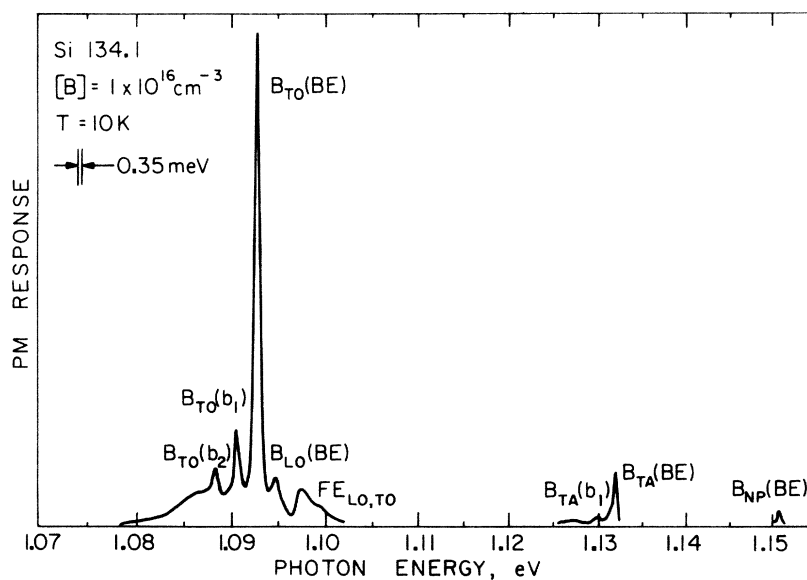


FIG. 1. Liquid-He photoluminescence spectrum of B-doped Si. The peak energies of the lines are listed in Table I while the notation is explained in the text.

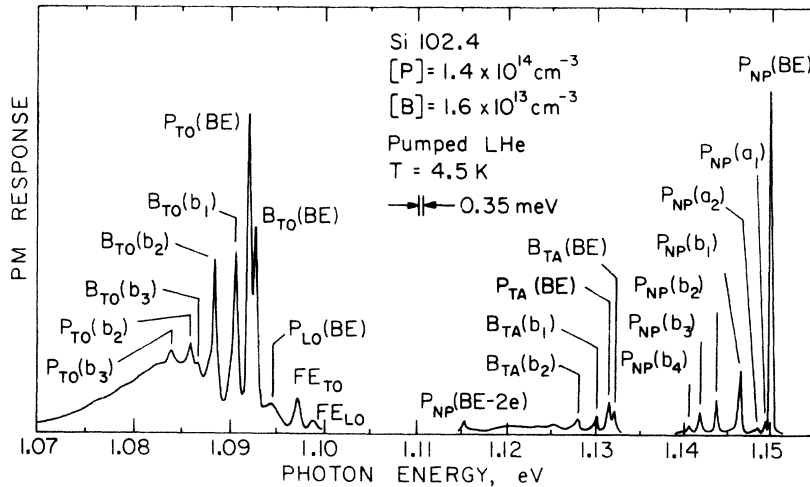


FIG. 2. Photoluminescence spectrum of P-doped Si containing unintentional B impurities. See Tables I and II for peak energies.

(TO)], were calculated from the absorption thresholds<sup>3</sup> using a TO energy of 58.0 meV derived from Tables I and II. The B peaks are not plotted since their energies are nearly coincident with those of Li, a fact which may be related to the weak binding of excitons to both Li and B.

We conclude that the center responsible for the Li lines is the isolated interstitial donor and not the Li-O complex. This is shown by the fact that the observed energy of the Li BE agrees with Haynes's rule<sup>6</sup> when the Li ionization energy of 33 meV, as opposed to the Li-O energy of 39 meV,<sup>19</sup> is used. In addition, we expect some NP component in the PL spectra if the center is Li-O since its donor ionization energy is near that of Sb for which  $Sb_{NP}(BE)/Sb_{TO}(BE) = 0.03$ ,<sup>5</sup> whereas we observe that  $Li_{NP}(BE)/Li_{TO}(BE) < 0.0016$ . Photoluminescence of Si diffused with Li enriched to ~96% Li<sup>6</sup>, instead of Li with natural isotopic abundance (~93% Li<sup>7</sup>), was also studied but no isotope shifts were observed in any of the Li lines.

Figures 1-3 show that the *b* lines must be due to radiative decay of an electron and hole, both of which are bound in a complex at an impurity. An impurity is involved since the *b* lines are only seen when a donor or acceptor is present and its BE line observed. In addition, the relative strength of the NP component is the same as the BE with which the *b* lines are related. Since the *b* lines show no thermal broadening as does the FE, the electron and hole must be immobile and bound to an impurity. Within experimental error the lines have the same full width at half-maximum as the BE with the TO components being ~0.4 meV in width while the NP BE and *b* lines of P were resolution limited at <0.14 meV. Finally, we note that contrary to the interpretation of Pokrovskii,<sup>15</sup> the *b* lines do not broaden and merge to form a broad band, but as Fig. 2 shows they appear to be superimposed on the band. We also observe that in Fig. 3 the Li lines have an underlying background which appears to peak at a slightly higher energy than the band in

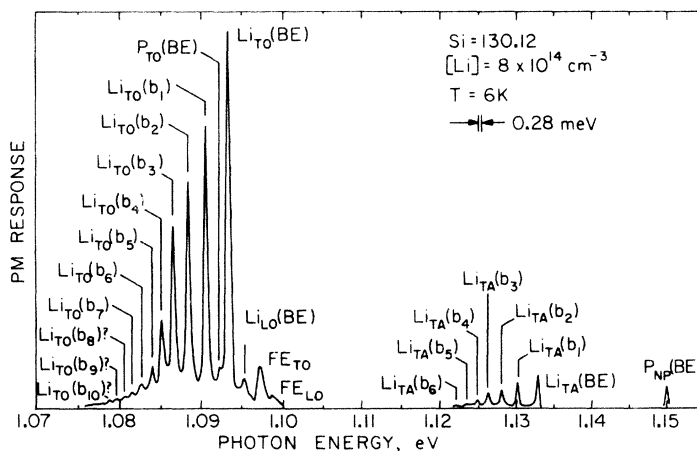


FIG. 3. Liquid-He photoluminescence spectrum of Li-doped Si. Bound-exciton lines due to P, whose concentration was established to be  $7 \times 10^{12} \text{ cm}^{-3}$  from a resistivity measurement before Li diffusion, are also detectable.

TABLE I. Peak energies of the observed B lines. Each entry, except for one superscripted with \*, is the mean of several measurements ( $\pm$  one standard deviation).

Transition	Peak energy (eV)			
	NP	TA	LO	TO
BE	1.1507* $\pm 0.0002$	1.13167 $\pm 0.000067$	1.09447 $\pm 0.000066$	1.09265 $\pm 0.000038$
$b_1$		1.12955 $\pm 0.000086$		1.09040 $\pm 0.000029$
$b_2$		1.12743 $\pm 0.00012$		1.08810 $\pm 0.000042$
$b_3$				1.08653 $\pm 0.000089$

Fig. 2.

The  $b$  lines are only observed below  $\sim 10$  K, whereas the BE have been detected up to  $\sim 30$  K. The PL of Si with  $7 \times 10^{15}$  Li/cm<sup>3</sup> cooled by He gas to 20 K shows only the FE and Li BE (Fig. 5) while at 7 K the spectrum was similar to that in Fig. 3. Similar behavior was observed for the P- and B-doped samples. At liquid-He temperatures the Li spectrum showed only minor changes with temperature. Immersed in pumped liquid He at 1.9 K instead of 4.2 K, the Hg arc spectrum of the sample in Fig. 3 decreased as a whole to  $\sim 60\%$  of its original intensity while the FE fell to  $40\%$ . With GaAs-laser excitation the same temperature change caused the FE and BE to decrease to  $\sim 80\%$  while the  $b$  line intensities were nearly unchanged.

Plotted in Fig. 6 is the intensity of the TO component of the  $b$  lines (in percent of the BE) as a

TABLE II. Peak energies of the observed P lines. Each entry is the mean of several measurements with the error being one standard deviation. The averages of the phonon energies deduced from Tables I and II are ( $\pm$  one standard deviation)  $E_{TA} = 19.0 \pm 0.17$ ,  $E_{LO} = 56.1 \pm 0.17$ , and  $E_{TO} = 58.02 \pm 0.057$  meV.

Transition	Peak energy (eV)			
	NP	TA	LO	TO
BE	1.14992 $\pm 0.000018$	1.13104 $\pm 0.000068$	1.09403 $\pm 0.000047$	1.09196 $\pm 0.000025$
$a_1$	1.1488 $\pm 0.0001$			
$a_2$	1.14795 $\pm 0.00005$			
$b_1$	1.14633 $\pm 0.000046$			1.08818 $\pm 0.000037$
$b_2$	1.14368 $\pm 0.000056$			1.08558 $\pm 0.000035$
$b_3$	1.14148 $\pm 0.000078$			1.08365 $\pm 0.000029$
$b_4$	1.14025 $\pm 0.00015$			
BE-2e	1.11492 $\pm 0.000054$			

TABLE III. Peak energies of the observed Li lines. Each entry is the mean ( $\pm$  one standard deviation) of several measurements and doubtful lines are indicated by a question mark.

Transition	Peak energy (eV)		
	TA	LO	TO
BE	1.13262 $\pm 0.000052$	1.09507 $\pm 0.000024$	1.09321 $\pm 0.000022$
$b_1$	1.12993 $\pm 0.000041$		1.09047 $\pm 0.000020$
$b_2$	1.12783 $\pm 0.000041$		1.08823 $\pm 0.000016$
$b_3$	1.12596 $\pm 0.000065$		1.08642 $\pm 0.000019$
$b_4$	1.12460 $\pm 0.000050$		1.08503 $\pm 0.000031$
$b_5$	1.1232 $\pm 0.00010$		1.08383 $\pm 0.000029$
$b_6$	1.1220 $\pm 0.0002$		1.08252 $\pm 0.000073$
$b_7$			1.08107 $\pm 0.000033$
$b_8$			1.0804 ? $\pm 0.0001$
$b_9$			1.0792 ? $\pm 0.0002$
$b_{10}$			1.0784 ? $\pm 0.0002$

function of the Li concentration. The PL of each of the four samples was done under similar conditions of excitation and temperature. Since the peaks are superimposed on a background (cf. Fig. 3 from which the points at  $8 \times 10^{14}$  cm<sup>-3</sup> were taken), their peak heights were measured from a baseline established by connecting the minima between peaks with a straight line. The general trend is a decrease in intensity with the lower-energy lines decreasing faster as the Li increases. The integrated FE luminescence (which includes the LO and TO components because of difficulties in separating the two) also decreases at higher donor concentrations. This suggests that the primary effect of increasing the Li is to decrease the FE concentration through formation of BE and subsequent nonradiative Auger recombination.<sup>25</sup> If the  $b$  lines are dependent on the FE as well as the Li concentration, then their intensity can be expected to decrease along with the FE. Similar behavior has been observed for P concentrations in the  $7 \times 10^{12}$  to  $2 \times 10^{16}$  cm<sup>-3</sup> range and for B in the  $4 \times 10^{11}$  to  $1 \times 10^{16}$  cm<sup>-3</sup> range. We have also observed in both Li- and P-doped Si what seems to be a broadening, merging, and shifting of the  $b$  lines at  $\sim 4 \times 10^{17}$  -

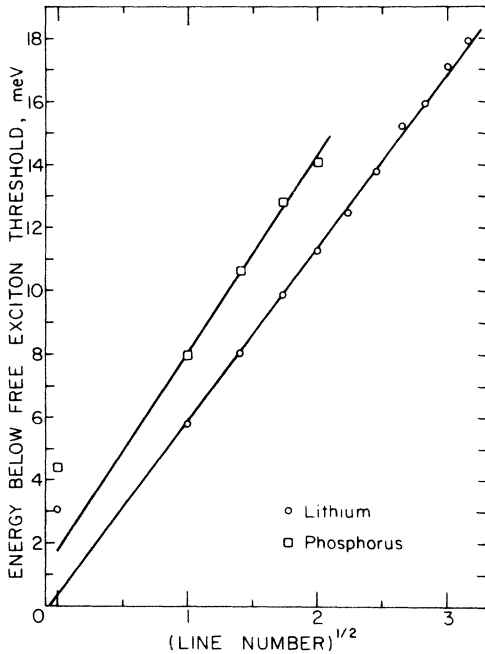


FIG. 4. Peak energies, relative to the FE emission threshold, of the P and Li lines vs the square root of the line number. The BE is taken as line zero. The last three Li lines are doubtful but have energies consistent with the rest of the data.

$\text{cm}^{-3}$  impurity levels. This effect was not studied as a function of concentration but it was noticed that the luminescence had the same temperature dependence as the  $b$  lines so that only the BE (which remained sharp) was seen at  $T \sim 20$  K.

The dependence of the  $b$  lines on excitation intensity was studied for both Hg arc and GaAs laser sources in a sample with  $3.5 \times 10^{14}$  Li/ $\text{cm}^3$  (Figs. 7 and 8). In both cases, the incident power was varied by attenuating with calibrated filters. The measured widths of the FE give sample temperatures (Fig. 7) of 6.7, 5.8, 6.1, and 6.4 K (all  $\pm 0.5$  K) as the excitation intensity is decreased, showing that heating effects are probably minimal. The most obvious difference between the 100 and 42% spectra is the large decrease in the background. This broad band is probably the same as that in Figs. 2 and 3, and its behavior here is additional evidence that it is not directly related to the  $b$  lines. The much higher intensity of the GaAs laser compared to the arc lamp is evident in the large broad band which dominates the top two spectra in Fig. 8. The FE widths for the upper three curves give temperatures of 6.9, 5.9, and 6.6 K ( $\pm 0.5$  K), indicating again that there are no large temperature variations. Comparing the 100% and 50% excitation curves, the broad band is seen to vary linearly with excitation, while everything else

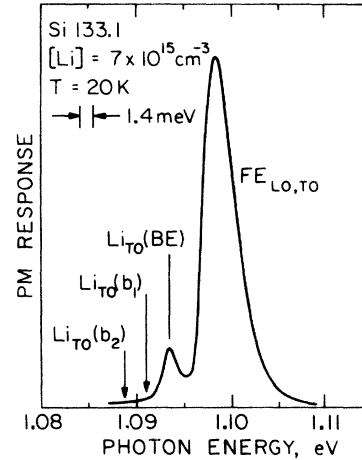


FIG. 5. The 20-K photoluminescence of Li-diffused Si. The liquid-He spectrum of this sample was similar to that in Fig. 3.

depends sublinearly.

An attempt to combine the results of Figs. 7 and 8 on one graph is shown in Fig. 9 where the Hg-arc excitation intensity was scaled relative to the GaAs excitation. This was done by plotting the ratio of FE to BE luminescence as a function of excitation intensity, then shifting the Hg-arc points until a single straight line fit both the arc lamp and laser data. After this, all of the Hg-arc points for the broad band (labeled ME), BE, FE, and  $b$  lines (not plotted) were scaled vertically by the same factor. The points for FE and ME represent the integrated intensity and include both LO and TO components since the two cannot be easily separated. The intensity of the sharp lines is represented by peak

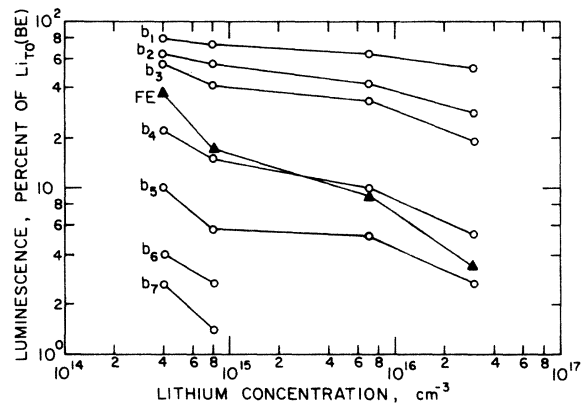


FIG. 6. Peak height of the Li  $b$  lines, in percent of the BE, as a function of Li concentration. The points for the FE are the integrated intensities of the LO and TO components, normalized to  $\text{Li}_{\text{TO}}(\text{BE})$  (arbitrary units).

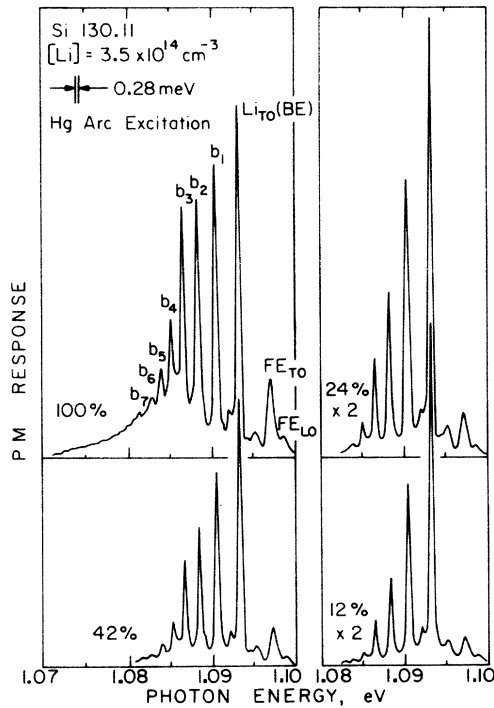


FIG. 7. Dependence of the Li spectrum on Hg arc excitation intensity. The relative excitation is indicated in percent and the two spectra on the right are taken at increased amplifier gain.

height above the underlying broad band, which was approximated by straight lines connecting valleys between lines. We emphasize that our experiments were not intended to distinguish between the ME and EHD mechanisms for the broad band and that the notation in the figures is for convenience only. It can be seen that  $I_{FE}/I_{BE}$ , the ratio of FE to BE luminescence, is a good measure of the excitation and from Fig. 9 it is estimated that the maximum Hg-arc generation rate is 2.7% of the maximum laser rate. The ME points also fit a straight line, while the BE and FE curves both show breaks, although the one for the FE is small and is not explicitly shown.

In Fig. 10 the data from Figs. 7 and 8 are again plotted but with  $I_{FE}/I_{BE}$  as the independent variable and the peak heights (less background) of the  $b$  lines and the integrated broad band luminescence, all normalized to the BE, as the dependent variables. This format has the advantage of being able to plot the arc lamp and laser data on one graph without the use of scaling parameters. The ME points fit a straight line with slope 2.0 while the  $b$  lines all exhibit changes in slope. This behavior clearly shows that the broad band and the  $b$  lines are not directly related. From the slopes in Table IV it is seen that in the low-excitation

regime the data obey the relation  $I_n/I_{BE} \propto (I_{FE}/I_{BE})^{n/2}$ , where  $I_n$  is the intensity of line  $b_n$ .

The luminescence of Si doped with  $3 \times 10^{16}$  Li/cm<sup>3</sup> is shown at different decay times after excitation by a GaAs laser (Fig. 11). The laser current was 3-A peak in a 2- $\mu$ sec pulse with a 4% duty factor. The times shown refer to when the 100-nsec aperture of the boxcar integrator opened. The top spectrum represents the steady-state situation since it is identical to those spectra taken earlier in the pulse. This can be compared with the 50% excitation spectrum of Fig. 8, which was recorded at nearly the same conditions except for a 2- $\mu$ sec aperture. The much higher Li concentration of the present sample is evident in the lower FE and broad-band background intensities. From the series of experiments in Fig. 11 it is evident that the broad band decays the fastest, the Li BE the slowest, while the  $b$  lines are intermediate.

The time dependence of the lines is shown in Figs. 12 and 13. Each curve was originally taken with the monochromator (at the same resolution as in Fig. 11) set to the peak of that line and the boxcar aperture scanned in time. The processed signals from the integrator were linearly recorded

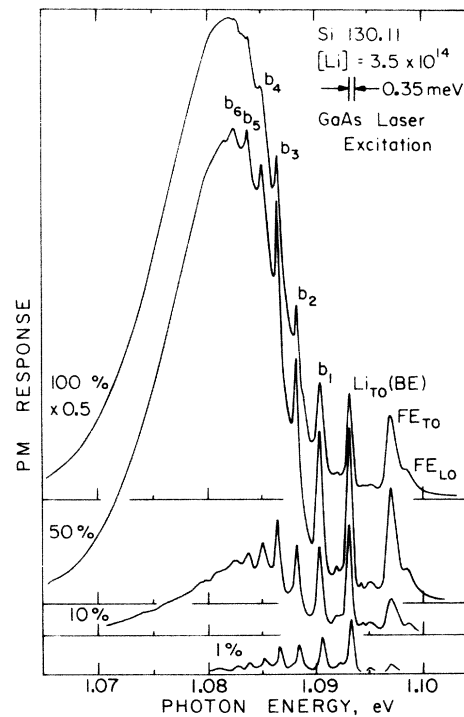


FIG. 8. Dependence of the Li spectrum on GaAs-laser excitation intensity. The relative excitation is indicated in percent and the top spectrum was taken at decreased amplifier gain. The laser current was 6-A peak in a 2- $\mu$ sec pulse at 4% duty factor.

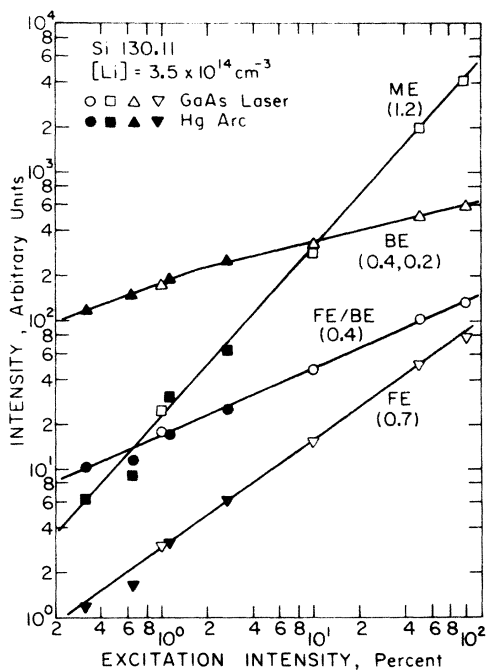


FIG. 9. Intensity of the FE, ME, BE and FE normalized to the BE vs excitation. The intensity of the Hg arc relative to the laser was determined by shifting horizontally the arc data until the FE/BE points fit a single line. The arc points were then shifted vertically until the ME data fell on a straight line. The FE and ME points are in the same units, but cannot be compared with those for the BE. The slopes are indicated in parentheses.

and replotted by hand into the displayed format. The laser current, which was the same in magnitude and duty factor as in Fig. 11, was recorded by the boxcar at the same settings as the spectra. The pulse width at one-half peak current was determined to be  $2.03 \mu\text{sec}$  and is shown in the figures. The times at which the current was 1% of peak were  $0.03$  and  $2.39 \mu\text{sec}$ , and the 10–90% rise and fall times were both  $200 \text{ nsec}$ . The delay time in the photomultiplier signal processing electronics was measured to be  $60 \text{ nsec}$ , excluding transit time in the RCA 7102. The transit time is unknown but estimated to be much less than  $40 \text{ nsec}$ . Therefore the curves of Figs. 12 and 13 should be shifted toward  $t = 0$  by  $\sim 100 \text{ nsec}$ , but it is seen that they are still delayed with respect to the laser current.

The time behavior of the lines agrees with the conclusion from Fig. 11 that the Li BE has the longest decay time. The different decay rates of the background and the  $b$  lines show as a change in slope. The initial and secondary time constants are summarized in Table V where it is seen that the initial time constants, which are due to the decay of the underlying broad band, decrease ap-

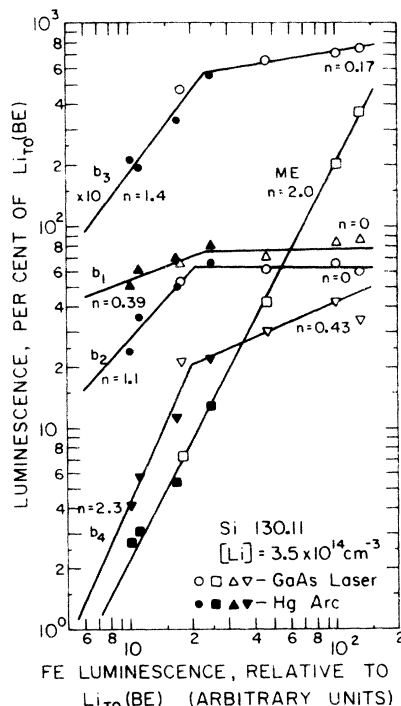


FIG. 10. Normalized luminescence of the  $b$  lines and the broad band (labeled ME) as a function of normalized FE luminescence. Since everything is normalized to  $\text{Li}_{T0}(\text{BE})$ , no scaling parameters are required as in Fig. 9. The points for  $b_3$  have been shifted upwards by a factor of 10. The points for ME are in the same units as the FE, but are moved down by a factor of 20. The  $n$  values are the slopes of the lines.

proximately linearly with line number. This behavior is consistent with Pokrovskii's observation that the peak of the broad band shifted to lower energies with increasing excitation.<sup>12–15</sup>

There is a noticeable delay in the rise of the luminescence in Figs. 12 and 13. Measuring from the one-half peak signal points, the BE is shifted  $\sim 150 \text{ nsec}$  with respect to the  $b$  lines. Similar experiments were done on Si with  $3.5 \times 10^{14} \text{ Li/cm}^3$ , but the large background (cf. Fig. 8) made it impossible to obtain good data. The delay effects were not noticed in this case, but the decay times

TABLE IV. Slopes of the normalized  $b$ -line intensity vs normalized FE intensity curves of Fig. 10.

Line number	Slope	
	Low excitation	High excitation
1	0.39	0
2	1.1	0
3	1.4	0.17
4	2.3	0.43

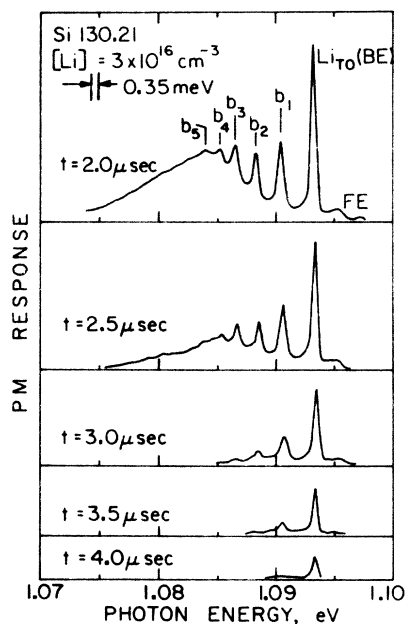


FIG. 11. Time decay of the Li spectrum following pulsed GaAs-laser excitation. Laser current was 3-A peak in a 2- $\mu$ sec pulse at 4% duty factor. Times are the same as in Figs. 12 and 13.

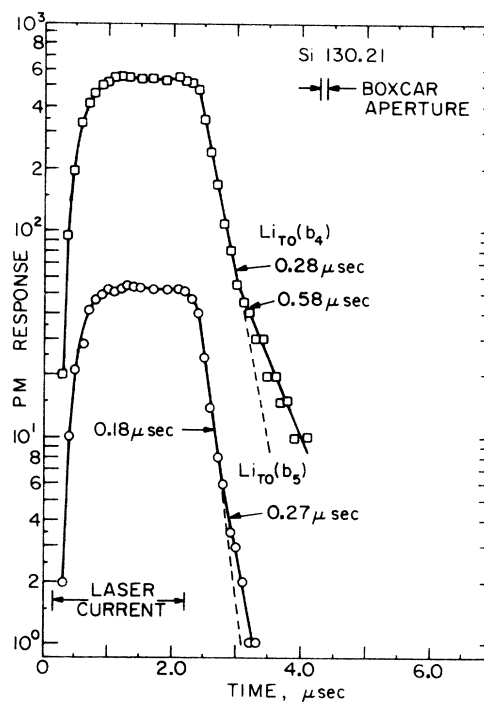


FIG. 13. Time decay of the Li lines  $b_4$  and  $b_5$ . Experimental conditions are the same as in Figs. 11 and 12. The curve for  $b_4$  has been shifted upwards by a factor of 10.

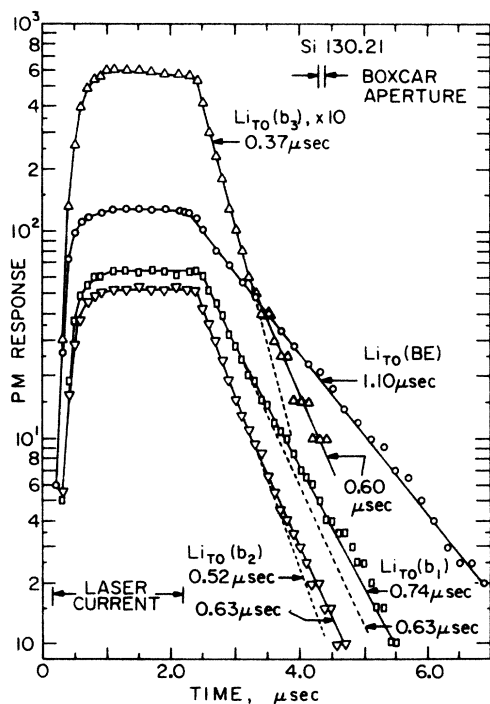


FIG. 12. Time decay of the Li BE and  $b$  lines. Experimental conditions are the same as in Figs. 11 and 13. The laser current pulse width at one-half peak is indicated. The curve for  $b_3$  has been shifted upward by a factor of 10.

were consistent with those in Figs. 12 and 13 with the FE having a time constant of 0.4  $\mu$ sec. The NP phosphorus lines (in the sample of Fig. 2) were obscured, but the signals were small and noisy since most of the luminescence was in the broad band. The decay time of the BE was 600 nsec, those of  $b_1$ ,  $b_2$  and the FE were 300 nsec. No decay effects were observed.

TABLE V. The  $1/e$  decay times of the Li BE and  $b$  lines. The  $b$  lines show an initial rapid decay due to the underlying background, followed by a slower secondary decay characteristic of the lines themselves. The secondary decay time of  $b_5$  is questionable since it is much shorter than those of lines 1-4 and the intensity of  $b_5$  is a very small portion of the total signal (cf. Fig. 11).

Line number	Initial ( $\mu$ sec)	Secondary ( $\mu$ sec)
0 (BE)	...	1.10
1	0.63	0.74
2	0.52	0.63
3	0.37	0.60
4	0.28	0.58
5	0.18	0.27 ?



## IV. DISCUSSION

## A. Summary of experimental results

On the basis of the experiments reported here and by others, the following statements about the *b* lines can be made.

1. *They are due to the radiative recombination of an electron and hole, both of which are bound to a donor or acceptor.* The lines have been observed for B, P, and Li, but not for In which was, however, studied in one sample only. Only bound immobile particles can be involved in the transitions since all of the lines are observed to be sharp, their widths being much less than the FE and comparable to BE linewidths. The electron and hole are bound to an impurity because the *b* lines are present only when the sample is doped and the BE emission at the associated donor or acceptor is simultaneously observed. In addition, the ratio of the relative strengths of the NP components of the *b* lines to that of their phonon replicas is the same as the corresponding ratio for the related BE.

The impurity giving rise to the *b* lines is isolated and unpaired, ruling out donor-acceptor pairs (both distant and nearest-neighbor associates). This is because diffusing samples with Li was sufficient to cause the lines to appear. If another center were also necessary, it would have to be present in concentrations up to  $10^{16} \text{ cm}^{-3}$  since the luminescence has been observed in Si containing B, P, or Li in those amounts. Also the same "coactivator" would be required to pair with a substitutional acceptor (B) as well as with a substitutional (P) or interstitial (Li) donor.

Finally we eliminate randomly distributed Li-Li, B-B, or P-P pairs (or higher aggregates) binding a single exciton in a manner analogous to that for the well-known NN lines in GaP.<sup>25</sup> Such luminescence would be strongest at high impurity concentrations (NN lines are dominant at N concentrations of  $10^{18} \text{ cm}^{-3}$  and above in GaP),<sup>26</sup> whereas the *b* lines are very prominent at  $10^{14} \text{ cm}^{-3}$  doping levels. In addition, one would expect the intensity of such pair lines to increase dramatically relative to the simple BE at high-impurity concentrations, again contrary to our observations (Fig. 6). Furthermore, (see below) the observed energy pattern is inconsistent with that expected for a random distribution of pairs.

2. *The *b* lines are not directly related to the broad band underlying them.* Our observations agree with previous reports that the broad band grew and shifted with increasing excitation intensities until its peak coincided with that due to the EHD.<sup>12-15</sup> We have not studied this broad band in detail and therefore cannot distinguish between the EHD and ME mechanisms. The band is, however,

distinct from the *b* lines in its excitation dependence, time decay and lack of an NP component.

3. *The *b* lines are observed for  $T \lesssim 10 \text{ K}$ , but very weakly or not at all above 15 K where the BE remains detectable.* As previously noted there are no large changes in the relative intensities of the *b* lines when the sample is immersed in pumped instead of normal liquid helium. This is not unexpected since the energy spacing between lines is much larger than  $kT$ . Unfortunately, no conclusion can be made about whether or not there is thermalization among the lines and it can only be stated that their temperature behavior is basically different from that of the BE.

4. *The energy by which line  $b_n$  is displaced below the FE threshold is proportional to  $n^{1/2}$ .* This rules out a number of possible mechanisms for the luminescence. Among these are donor-acceptor pair recombination, which has a well-characterized spectrum consisting of sharp lines that are irregular in their intensities and spaced in energy in a unique pattern<sup>27</sup> different from that observed for the *b* lines; bound-exciton two-electron transitions in which a BE decays and leaves the neutral impurity in an excited electronic state,<sup>5</sup> since the observed *b* lines spacings are inconsistent with those of either a rydberg series ( $\propto n^{-2}$ ) or the energy levels of Li, B, and P as known from excitation spectroscopy<sup>19,28,29</sup>; transitions in which a BE decays and leaves the ground electronic state in an excited vibrational (harmonic oscillator,  $\propto n$ ), or rotational (rigid rotor,  $\propto n[n+1]$ ) energy level; and mechanisms similar to that of the NN pair lines which in GaP are widely spaced at low photon energies and merge together as the BE line is approached.<sup>26</sup>

5. *No isotope shift has been observed for either the Li BE or *b* lines.* In CdS no shift was reported in the BE emission of Li acceptors, although a shift of about 0.18 meV was observed in the distant pair lines due to the Li acceptor and an unidentified double donor.<sup>30</sup> The explanation offered was that an isotope shift could be observed only if the transition affected the zero-point vibrational energy of the Li atom. Since the donor-acceptor pair transition involved a change in charge state of the Li acceptor, it was argued that this change affected the Li-host bonds (i. e., the spring constant for the vibrating Li atom) and consequently the impurity's zero-point energy. The BE decay on the other hand caused little charge redistribution around the Li so that no observable shift occurred. It is probable that this is the reason we detected no isotope effects. Such arguments are consistent with the fact that Li in Si is a nearly ideal donor with almost no central-cell corrections. In any case the lack of isotope effects in the *b* lines rules out their being due to transitions involving impurity

vibrations.

6. *The Zeeman splitting of the first B b line is different from that of the BE.* In PL studies of B-doped Si immersed in liquid He, Cherlow has observed the Zeeman splitting of  $B_{TO}(BE)$  and  $B_{TO}(b_1)$  at 91.6 kG.<sup>31</sup> Although the splittings were not analyzed in detail, he did note that the BE line appeared to split into three thermalized components while the  $b_1$  line split into three components whose intensities increased for the higher photon energy lines.<sup>31</sup> This difference in behavior shows that the electronic transition responsible for this line is not the same as for the BE. Vibronic transitions in which the BE decays and simultaneously excites a local mode or emits a phonon are therefore excluded.

7. *In previous studies of BE absorption done at 1.9 K on samples containing about  $10^{17} \text{ cm}^{-3}$  donors or acceptors, no absorption due to the b lines was reported.* Absorption would not be expected if the  $b$  lines were due to an exciton decaying within a multiexciton complex because such centers are highly excited states occurring only at large generation rates (Ref. 7). (However, it is also possible that the absence of absorption is due to the relatively high impurity concentrations used, since we have observed what appears to be a broadening and merging of the lines at these doping levels. On the other hand, our experiments demonstrate that the  $b$ -line photoluminescence is proportional to FE concentration, whereas high impurity density and the low excitation at which absorption is performed both give small FE concentrations.) An alternative explanation for the absence of absorption is that the  $b$  lines are caused by a splitting in the ground state and that only the lowest energy level is populated because of the temperature. This model, however, explains only the negative absorption result and is inconsistent with points 10 and 11.

8. *The b lines appear to shift, broaden, and merge while the BE remains sharp at impurity concentrations near  $10^{17} \text{ cm}^{-3}$ .* Since we have not carefully studied samples with dopings between  $10^{16}$  and  $10^{17} \text{ cm}^{-3}$ , it is premature to state that the observed bands are due to the  $b$  lines at these concentrations. If in fact they are, then this shows that the spatial extent of the excited state giving rise to them is larger than that of the BE.

9. *The b lines depend on the FE as well as the impurity concentration.* As Fig. 6 shows the dominant effect of increasing the impurity concentration seems to be a decrease in the FE lifetime and steady-state density by more rapid conversion of FE's to BE's which results in a reduction of the  $b$ -line intensities. This interpretation is also supported by the excitation dependence.

10. *The lines have an excitation dependence dif-*

*ferent from the BE and their normalized intensities show a power-law dependence on the normalized FE luminescence, the exponent increasing almost linearly with line number.* From this we conclude that all of the  $b$  lines cannot arise by a decay from the same excited state with a fixed branching ratio since in this case they would show the same behavior with excitation.

11. *The b lines have different decay times which are less than the BE and decrease with increasing line number.* This shows that the BE or  $b_1$  state cannot be the excited state from which an exciton decays with fixed branching ratio into a number of ground states. For such a system, all lines would decay at the same rate since the reciprocal of the excited-state lifetime is the sum of the reciprocal lifetimes of the parallel decays.

12. *The rise of the b-line photoluminescence is delayed by approximately 150 nsec with respect to the BE.* This effect was observed in a sample with  $3 \times 10^{16} \text{ cm}^{-3}$  Li atoms but not in one doped to  $3.5 \times 10^{14} \text{ cm}^{-3}$ . Besides the delay phenomenon, another difference between these two samples was that the FE and the broad band beneath the  $b$  lines were stronger in the spectra of the lower doped one. The observed delay shows that the  $b$  lines cannot be due to a transition which begins with the same excited state as the BE. The fact that no delay was observed at the higher FE concentrations of the low Li concentration sample further emphasizes our previous conclusions (points 9 and 10) that the  $b$  lines are more strongly dependent on the FE density than is the BE.

In summary we have ruled out a number of possible models. The conclusion that the  $b$  lines are associated only with a single unpaired impurity means that they cannot be due to donor-acceptor pairs, or cooperative effects between two centers such as the undulation spectra of GaP.<sup>32,33</sup> The energy spacing of the lines shows that they cannot be caused by hydrogenic, harmonic oscillator, or rigid rotor energy states. This excludes models which involve bound-exciton two-electron and vibronic transitions, for example. The excitation and time decay show that the lines cannot arise from a single excited state decaying into a number of ground states.

#### B. Possible models

From the discussion of Sec. IV A the only models left to consider are those which involve multiple excited states of a single center, and models in which each line is due to a different center.

##### 1. Multiple excited states

Consider, for example, an exciton bound to an impurity, but with the possibility of the complex being in one of several electronic states whose en-

ergy spacings correspond to that of the  $b$  lines. This model allows different luminescent decay times for each  $b$  line since the decay time of each line would depend only on the lifetime of the excited state. Assuming that the excited states have the same degeneracy, that all transitions are allowed, and that the states are in thermal equilibrium, the intensity of each line should decrease with increasing photon energy because of thermalization. However, the opposite is observed for the  $b$  lines. This implies that if this model is correct, the degeneracies, transition probabilities, or radiative efficiencies of each state must increase strongly with decreasing line number. In addition, one would expect the higher energy lines to increase in intensity as the temperature is raised, whereas only the BE is observed for elevated temperatures. At a constant temperature the entire spectrum should increase uniformly with excitation since the relative intensities of the lines would be fixed by Maxwell-Boltzmann probabilities. Again this is in disagreement with experiment. These considerations lead to the conclusion that in order for this hypothesis to be valid the excited states cannot be in thermal equilibrium. The model also predicts that the  $b$  lines should be observable in absorption, contrary to the experiments.

## 2. Multiexciton complexes on independent centers

Since it has been argued previously that the centers responsible for the  $b$  lines must be isolated, two-center mechanisms such as those proposed for the undulation spectra in GaP are invalid.<sup>32,33</sup> The high symmetry of Si and the large number of observed Li  $b$  lines rule out the possibility of each different line being caused by the isolated impurity occupying a different lattice site. The power-law dependence of the lines on normalized FE intensity suggests multiexciton complexes bound to neutral donors or acceptors. Figure 14 shows the energy levels and radiative transitions which will be assumed for this model. The transition energy corresponding to line  $b_n$  is

$$E_n = E_{gx} - \delta E_n, \quad (1)$$

where line number zero is the BE,  $E_{gx}$  is the exciton band gap, and  $\delta E_n$  is the quantity plotted in Fig. 4. According to this model line  $b_n$  arises from the radiative decay of one exciton in a complex consisting of  $n+1$  excitons bound to a neutral donor or acceptor. This results in the emission of a photon of energy  $E_n$  and leaves a complex containing  $n$  excitons. The quantity  $\delta E_n$  represents the binding energy of one FE at rest to an  $n$ -exciton complex. The total binding energy of an  $(n+1)$ -exciton complex, relative to  $n+1$  noninteracting excitons at rest, is

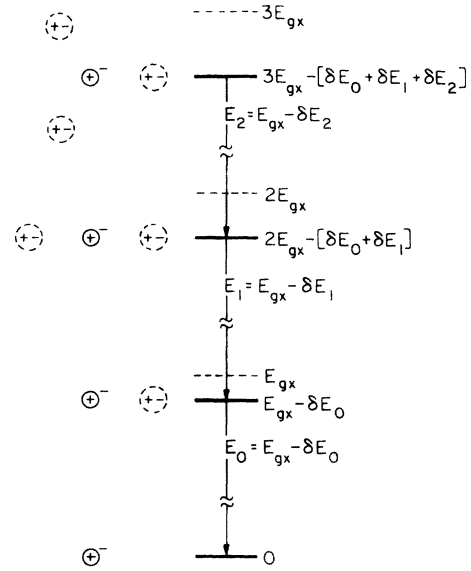


FIG. 14. Energy levels and radiative transitions (without phonon emission) responsible for the  $b$  lines in the multiexciton complex model. The drawing is not to scale since the  $\delta E_n$  are actually much smaller than  $E_{gx}$ . To the left of each energy level the complex is schematically indicated with the positively charged donor core in a solid circle and the exciton in the dotted. The bottom transition is the BE decay.

$$E_B(n) = \delta E_0 + \delta E_1 + \dots + \delta E_n. \quad (2)$$

As was demonstrated in Fig. 4,  $\delta E_n$  is proportional to  $n^{1/2}$  so that for large  $n$

$$E_B(n) \cong b \int n^{1/2} dn = \left(\frac{2}{3}\right) bn^{3/2}. \quad (3)$$

From the energy diagram it can be seen that

$$\delta E_n = E_B(n+1) - E_B(n) = \frac{2}{3} b [(n+1)^{3/2} - n^{3/2}] \quad (4)$$

which, when a series expansion of  $(1+1/n)^{3/2}$  is made, results in

$$\delta E_n = b(n + \frac{1}{2})^{1/2} + O(n^{-3/2}). \quad (5)$$

The maximum error due to ignoring terms of order  $n^{-3/2}$  in (5) occurs for  $n=0$  when the approximation gives a value of  $0.707b$  instead of  $2b/3$  which Eq. (4) predicts.

Figure 15 shows a least-squares fit to the peak energies  $E_n$  in Tables I, II, and IV by the function

$$E_n = E_{FE}(\text{effective}) - b(n + \frac{1}{2})^{1/2}. \quad (6)$$

The deduced values of  $E_{FE}$  (effective) and  $b$  are 1.09756, 1.09659, and 1.15495 eV and 5.29, 5.17, and 7.10 meV for Li, B, and P, respectively. It is interesting to note that the BE energies (line number zero) do not deviate a large amount from

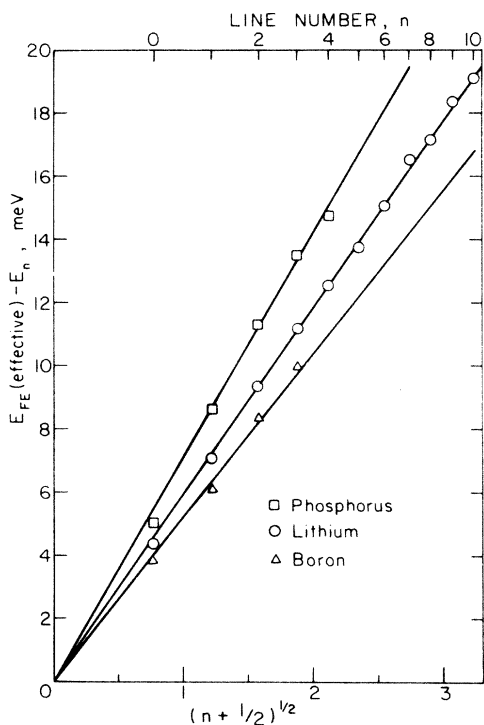


FIG. 15. Least-squares fit of the experimental Li, B, and P BE and  $b$ -line peak energies to the function (represented by straight lines)  $E_n = E_{FE}(\text{effective}) - b(n + \frac{1}{2})^{1/2}$ . The last three Li lines are questionable, but have been included in the calculation.

this hypothetical law and that  $E_{FE}(\text{effective})$  for Li and P agree well with the TO and NP FE emission thresholds of  $1.0978 \pm 0.0004$  eV and  $1.1551 \pm 0.0003$  eV calculated from the TO phonon and absorption threshold energies of Ref. 3. The least-squares fit to the B data, however, yields a value closer to the 1.0963 eV arrived at by using a TO energy of 58.0 meV and the Shaklee and Nahory absorption threshold.<sup>3</sup> For Li and P it seems that  $b$  may depend linearly on ionization energy, if one assumes  $b$  is zero at zero ionization energy.

The kinetics of this model can be very complicated. In the simplest approximation  $N_k$ , the concentration of  $k$  exciton centers, has loss due to the radiative recombination of an exciton (adding to  $N_{k-1}$ ) and to the trapping of a free exciton (adding to  $N_{k+1}$ ), and gain due to the decay of an exciton in a  $(k+1)$ -exciton center and to the trapping of an exciton by a  $(k-1)$ -exciton complex. More complete treatments would include thermal ionization of excitons and Auger processes. With the present data too many assumptions would be required for a meaningful theoretical calculation of the excitation dependence, but it can be seen that in terms of chemical reaction kinetics one would expect a

$k$ -exciton complex to exhibit  $k$ th-order kinetics with respect to FE concentration, which is qualitatively what appears to be happening in Fig. 10 where  $I_n/I_{BE} \propto (I_{FE}/I_{BE})^{n/2}$ .

It is possible that the delay with respect to the BE in the rise of the  $b$ -line photoluminescence is a consequence of the nature of the binding of the multiexciton complex. Since the  $H^-$ -like center consisting of a donor core with two bound electrons is known to be stable,<sup>34</sup> the rapid rise of the BE luminescence could be a result of BE being quickly formed through sequential capture of electrons and holes. On the other hand, multiexciton complexes, because of the detailed nature of their binding, conceivably could not exist in a charged state and instead of sequentially capturing electrons and holes must directly capture FE. The FE capture is expected to be a slow process, thus contributing to the delay in the  $b$ -line PL, since only neutral species are involved. An additional factor in the delay could be a slow increase in the FE concentration due to competition between the FE and BE formation processes for electrons and holes.

Finally, it is seen that the multiexciton complex model also explains the lack of absorption since in order for line  $b_n$  to be observed the  $n$ -exciton centers must be present in appreciable amounts. This would not be the case under the low excitation conditions at which absorption experiments are performed.

## V. CONCLUSION

We have performed the first detailed study of sharp, impurity-related photoluminescence lines which were originally hypothesized to be due to nucleation of electron-hole liquid drops.<sup>12-15</sup> These lines are a general effect since they have been observed with three very different types of impurities: Li, an interstitial species and the shallowest donor in Si; P, a group-V substitutional donor with significant central-cell effects; and B, the shallowest substitutional acceptor. The peak energy of line  $b_n$  fits the law  $E_n = E_{FE}(\text{effective}) - b(n + \frac{1}{2})^{1/2}$ , where the values of the intercept and slope depend on the impurity. Because of this behavior models involving two impurities separated by discrete lattice spacings, harmonic oscillators, rigid rotors, or hydrogenic energy levels have been discarded. We have eliminated models with a single excited state decaying into a number of ground states since the lines exhibit different excitation dependence and decay times. The excitation behavior of the lines leads to the conclusion that if they are due to excited state splittings, they cannot be in thermal equilibrium. The most consistent hypothesis is multiexciton complexes where line  $b_n$  is caused by the radiative decay of an exciton bound in an  $(n+1)$ -exciton complex resulting

in emission of a photon and leaving an  $n$ -exciton center. The binding mechanism of the complexes is not understood, but for Li and P the parameter  $b$  in  $E_n = E_{FE}(\text{effective}) - b(n + \frac{1}{2})^{1/2}$  appears to increase linearly with the ionization energy of the impurity, which is analogous to Haynes's rule for simple BE. Photoluminescence of other donors and acceptors needs to be studied in order to establish the exact nature of this trend which may be intimately related to the central-cell forces. Measurement of the temperature behavior of the  $b$  lines could further confirm the nature of the complexes.

Finally it is noted that these bound complexes could be intermediates in the nucleation of liquid electron-hole drops in Si. If so, it is to be expected that as the bound complex grows in size the relative binding energy of the complex to the fixed impurity decreases until at some specific size the complex can be detach itself from the impurity and become a free embryonic electron-hole drop.

#### ACKNOWLEDGMENT

The authors are grateful for the interest of T. N. Morgan who suggested the multiexciton-complex model and the energy fits shown in Figs. 4 and

15 and discussed in Eqs. (1)–(6).

*Note added in manuscript.* After this manuscript was completed the work of R. Sauer [Phys. Rev. Lett. **31**, 376 (1973)] came to our attention. He has studied in B- and P-doped Si what we have designated the  $b$  lines, and because of the energy spacings of the lines and dependence on excitation intensity and impurity concentration, has arrived at the same model which we have. On the basis of five B and six P lines (including the BE) Sauer has fit the line energies,  $E_m$ , with the equation  $E_m - h\nu_{FE} = -18.5[1 - e^{-\alpha m}]$  meV, where  $m$  is the line number (with the BE as number one),  $h\nu_{FE}$  is the peak energy of the FE band, and  $\alpha$  is 0.21 for B and 0.31 for P. Since we have observed that the B and Li  $b$ -line energies are nearly coincident, we have used Sauer's equation for B to fit the Li energies. It is interesting to note that his equation does not fit the B BE energy, but that it does agree within 0.3 meV of our observed Li BE energy. However, for the  $m = 8$  line, Sauer predicts an energy which is too high by 0.8 meV, and the discrepancy increases to 1.9 meV for  $m = 11$ . We therefore believe that the square-root dependence is a better description of the line energies.

†Research sponsored by the Joint Services Electronics Program through the Air Force Office of Scientific Research/AFSC under contract F 44620-71-C-0067.

\*Present address: Philips Laboratories, Briarcliff Manor, New York 10510.

<sup>1</sup>G. G. MacFarlane, T. P. McLean, J. E. Quarrington, and V. Roberts, Phys. Rev. **111**, 1245 (1958).

<sup>2</sup>P. J. Dean, Y. Yafet, and J. R. Haynes, Phys. Rev. **184**, 837 (1969); Phys. Rev. B **1**, 4193 (1970).

<sup>3</sup>K. L. Shaklee and R. E. Nahory, Phys. Rev. Lett. **24**, 942 (1970).

<sup>4</sup>J. R. Haynes, M. Lax, and W. F. Flood, in *Proceedings of the International Conference on Semiconductor Physics, Prague*, 1960 (Academic, New York, 1961), p. 423.

<sup>5</sup>P. J. Dean, J. R. Haynes, and W. F. Flood, Phys. Rev. **161**, 711 (1967).

<sup>6</sup>J. R. Haynes, Phys. Rev. Lett. **4**, 361 (1960).

<sup>7</sup>P. J. Dean, W. F. Flood, and G. Kaminsky, Phys. Rev. **163**, 721 (1967).

<sup>8</sup>J. R. Haynes, Phys. Rev. Lett. **17**, 860 (1966).

<sup>9</sup>J. D. Cuthbert, Phys. Rev. B **1**, 1552 (1970).

<sup>10</sup>A. R. Hartman and R. H. Rediker, *Proceedings of the Tenth International Conference on the Physics of Semiconductors*, Cambridge, Mass., 1970, edited by S. P. Keller, J. C. Hensel, and F. Stern (U. S. AEC, Springfield, Va., 1970), p. 202.

<sup>11</sup>L. W. Keldysh, in *Proceedings of the Ninth International Conference on the Semiconductors*, Moscow, 1968 (Nauka, Leningrad, 1968), Vol. II, p. 1303.

<sup>12</sup>A. S. Kaminskii and Ya. E. Pokrovskii, Zh. Eksp. Teor. Fiz. Pis'ma Red. **11**, 381 (1970) [JETP Lett. **11**, 255 (1970)].

<sup>13</sup>A. S. Kaminskii, Ya. E. Pokrovskii, and N. V. Alkeev,

Zh. Eksp. Teor. Fiz. **59**, 1937 (1970) [Sov. Phys. - JETP **32**, 1048 (1971)].

<sup>14</sup>Ya. E. Pokrovskii, A. S. Kaminskii, and K. Svistunova in Ref. 10, p. 504.

<sup>15</sup>Ya. E. Pokrovskii, Phys. Status Solidi A **11**, 385 (1972).

<sup>16</sup>Ya. E. Pokrovskii and K. I. Svistunova, Fiz. Tekh. Poluprovodn. **4**, 491 (1970) [Sov. Phys. - Semicond. **4**, 409 (1970)].

<sup>17</sup>C. Benoît à la Guillaume, M. Voos, and F. Salvan, Phys. Rev. B **5**, 3079 (1972).

<sup>18</sup>W. F. Brinkman and T. M. Rice, Phys. Rev. B **7**, 1508 (1973). See also references therein and those cited by Refs. 15 and 17.

<sup>19</sup>R. L. Aggarwal, P. Fisher, V. Mourzine, and A. K. Ramdas, Phys. Rev. **138**, A882 (1965).

<sup>20</sup>A more detailed account of this work appears in Kenneth Kosai, Ph. D. thesis (University Microfilms, Ann Arbor, 1973).

<sup>21</sup>S. M. Sze and J. C. Irvin, Solid-State Electron. **11**, 599 (1968).

<sup>22</sup>Robert J. Spry and W. Dale Compton, Phys. Rev. **175**, 1010 (1968).

<sup>23</sup>Keiji Maeda, J. Phys. Chem. Solids **26**, 595 (1965).

<sup>24</sup>E. J. Bowen, J. Chem. Soc. **147**, 76 (1935). We have omitted the  $K_2Cr_2O_7$  which filters out the blue and uv light.

<sup>25</sup>D. F. Nelson, J. D. Cuthbert, P. J. Dean, and D. G. Thomas, Phys. Rev. Lett. **17**, 1262 (1966).

<sup>26</sup>D. G. Thomas and J. J. Hopfield, Phys. Rev. **150**, 680 (1966).

<sup>27</sup>D. G. Thomas, M. Gershenzon, and F. A. Trumbore, Phys. Rev. **133**, A269 (1964).

<sup>28</sup>A. Onton, P. Fisher, and A. K. Ramdas, Phys. Rev. **163**, 686 (1967).

- <sup>29</sup>R. L. Aggarwal and A. K. Ramdas, Phys. Rev. 140, A1246 (1965).
- <sup>30</sup>C. H. Henry, K. Nassau, and J. W. Shiever, Phys. Rev. B 4, 2453 (1971).
- <sup>31</sup>Joel M. Cherlow, Ph. D. thesis (Massachusetts Institute of Technology, 1972) (unpublished).
- <sup>32</sup>J. J. Hopfield, H. Kukimoto, and P. J. Dean, Phys. Rev. Lett. 27, 139 (1971).
- <sup>33</sup>T. N. Morgan, M. R. Lorenz, and A. Onton, Phys. Rev. Lett. 28, 906 (1972).
- <sup>34</sup>J. J. Hopfield, in *Proceedings of the Seventh International Conference on the Physics of Semiconductors*, Paris, 1964 (Dunod, Paris, 1964), p. 725.